

ABSORBING AREAS

We begin with a brief introduction to the concept of absorption in one and two dimensions, and then study an exemplary bifurcation sequence.

4.1 ABSORPTION CONCEPTS, 1D

We introduced in Chapter 2 the notions of critical points, which bound zones of multiplicity, and trapping intervals, which are mapped into themselves. These notions come together in the concept of an *absorbing interval*. This is an interval in the domain of the map which is trapping, is bounded by critical points, and is *super-attracting*, which means that every point sufficiently close to the critical endpoints will jump into the absorbing interval after a finite number of applications of the map.

In the context of an iterated map of an interval, the interesting dynamics take place within absorbing intervals. The critical points of a one-dimensional map determine absorbing intervals, and are useful in characterizing some bifurcations, especially those called global bifurcations. Examples of global bifurcations occur in Chapter 7.

4.2 ABSORPTION CONCEPTS, 2D

In two-dimensional iterations, we have a notion of *absorbing area*, generalizing the absorbing intervals of the one-dimensional case. The critical curves of a map of the plane play a role analogous

to that of the critical points of a one-dimensional map: they are useful in determining absorbing areas. We will now illustrate the role of critical curves in determining these important areas in which the interesting dynamics occur.

In this chapter we will study the first family of quadratic maps defined in the Introduction. We will now use the map of this family determined by $b = -0.8$ to illustrate the use of critical curves to determine an absorbing area.

Our map has two fixed points, P and Q . The *basic critical curve*, L , is the locus of points with “coincident preimages,” that is, the set of points having nearby points with different numbers of preimages or rank 1 (see Appendix 3, especially A3.2 – A3.3, for definitions). The *fundamental critical curve* L_{-1} is defined as the preimage of L . Thus, L is the image of L_{-1} under the map. Similarly, the *derived critical curve* L_1 is the image of L , and so on. All of these are called *critical curves*, as described in Chapter 2.

Note for those who have studied vector calculus: In the context of a generic smooth map, the fundamental critical curve L_{-1} will be a subset of the set of *critical points* in the Jacobian sense, points at which the Jacobian derivative of the map (a linear transformation) is degenerate (not a linear isomorphism), while the basic critical curve L is a subset of the set of *critical values* in the Jacobian sense. *Inflection points* are Jacobian critical points which do not belong to L_{-1} .

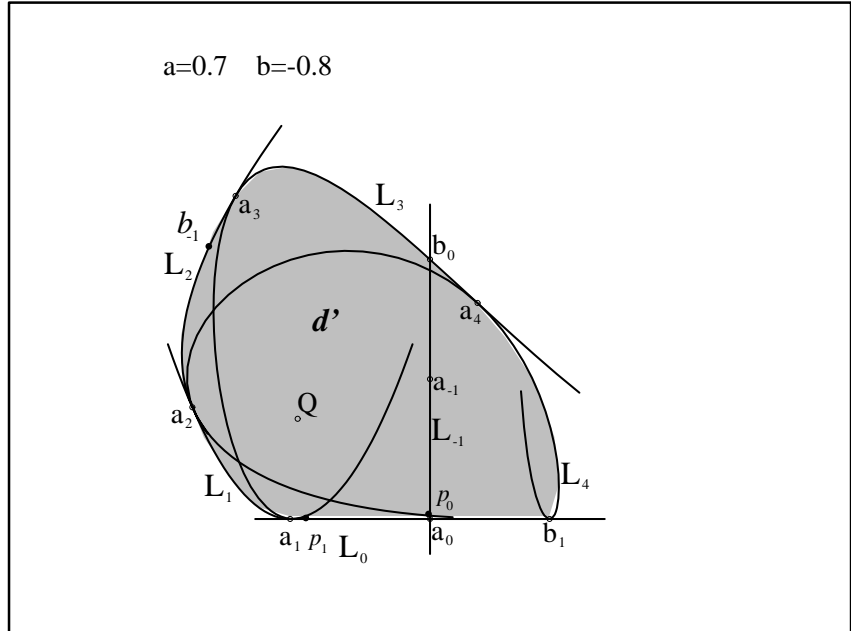
For this particular map, L_{-1} is the vertical axis, $x = 0$, and L is a horizontal line, $y = b = -0.8$. It will be convenient to choose a bounded interval in L_{-1} , S_{-1} , with endpoints a_{-1} , which is the origin $(0, 0)$, and a_0 , which is the image of a_{-1} under the map, the point $(0, -0.8)$.

Note: The critical curve denoted by L in the text is denoted by L_0 in the figures.

Figure 4-1 shows all these features and more. Note the points a_{-1} and a_0 , and the segments of L_{-1} , L , L_1, \dots, L_4 . As the map moves L_{-1} to L , and the point a_{-1} to a_0 , L is moved to L_1 , and the

FIGURE 4-1.

An absorbing area bounded by critical curves.



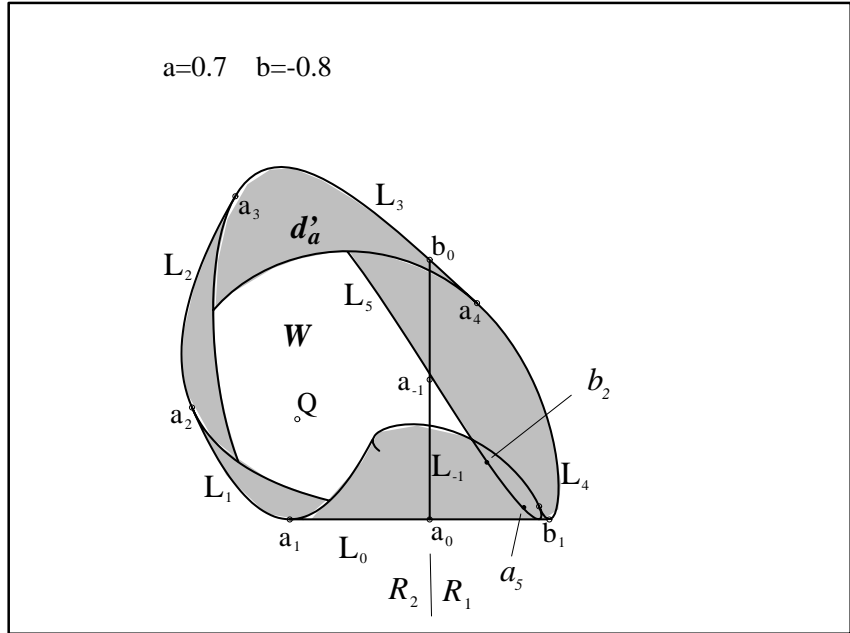
point a_0 to a point a_1 in L_1 . The transversal¹ (and here, indeed, orthogonal) crossing of L_{-1} and L at a_0 is transformed into a tangent contact of L and L_1 at a_1 . Then this point is mapped to a tangency of L_1 and L_2 at a_2 , and so on. Note that the curve L_2 crosses L_{-1} at the point p_0 , so L_3 is tangent to L at the point p_1 , the image of p_0 , and so on. Similarly, the curve L_3 crosses L_{-1} at the point b_0 , so L_4 is tangent to L at b_1 , the image of b_0 , and so on.

It is worthwhile to pause here and carefully study Figure 4-1. A point of transversal crossing of any curve, C , through L_{-1} is mapped into a point of tangency of the image of that curve, $f(C)$, with L . This is because of the *folding* which occurs as L_{-1} is mapped onto L . Also, a point of tangency of a curve C to the curve L_{-1} is mapped into a point of tangency of the image curve $f(C)$ and L .

1. An intersection of two curves is said to be *transversal* if they cross cleanly through each other in a single point, and are not tangent to each other.

FIGURE 4-2.

An annular absorbing area bounded by critical curves.



The action of the map may be visualized as a nonlinear folding of the plane at the fundamental critical curve, L_{-1} , followed by a nonlinear rotation moving L_{-1} to L around the point a_0 , and a nonlinear translation horizontally along L , so that a_{-1} ends up at a_0 . The critical curves shown in Fig. 4-1 are a kind of skeleton of the map, as we shall see.

Our next goal is to use these critical curves to discover an absorbing area of the map. By definition (see Appendix A3.5), an absorbing area is a region of the plane such that:

- it is mapped into (or onto) itself;
- its boundary is made up of segments of critical curves, or of limit points of an infinite sequence of critical curves; and
- it has a neighborhood every point of which eventually moves into the absorbing area.

As an example, note in Fig. 4-1 that the arcs b_1a_1 of L , a_1a_2 of L_1 , a_2a_3 of L_2 , a_3a_4 of L_3 , and a_4b_1 of L_4 bound a region d' ,

shown shaded in Fig. 4-1. This shaded region happens to be an absorbing area! First of all, it is invariant. For example, the segment a_4b_1 of L_4 is on the boundary of the region, d' , but the image of this arc, a_5b_2 , is internal to d' . This is clearly shown in Fig. 4-2, in which the image of a_4b_1 is indicated in L_5 .

Also, d' is absorbing: A point external to d' is mapped into d' in a finite number of iterations, as shown in Fig. 4-3, and this is the case for all points sufficiently near to d' .

Figure 4-2. also shows a shaded area, d'_a , bounded by the critical curve segments introduced in Fig. 4-1. It surrounds a hole, W , in which the fixed point Q is located. This is a smaller absorbing area, and is called an *annular absorbing area* for obvious reasons. Generally, absorbing areas may be topologically more complex, with many holes, and with many separate pieces.

Absorbing areas must contain attractors. One, d , is shown as a cloud of dots in Fig. 4-3. It is the attracting set of d' , and of the smaller absorbing area, d'_a , as well.

Usually there are smaller and smaller absorbing areas around any attractor of the map. All these, by definition, are bounded by critical arcs. And as they get smaller and smaller, but always enclose the same attractor, it is to be expected that the attractor itself is bounded by critical arcs, or by limit points of infinite sequences of critical arcs. Figure 4-4. shows 25 iterates of two intervals of L_{-1} , the two pieces of $d \cap L_{-1}$. These iterates bound the attractor shown in Fig. 4-3 quite closely.

Another basic concept of dynamics is the basin of attraction of an attractor. In the method of critical curves, we usually determine an absorbing area by the method illustrated above, and thus the attractor within it, and then determine the basin of attraction of the absorbing area. In Fig. 4-5 the basin of attraction, $D(d')$, is shown as the white region. Its boundary is made up of the repelling (nodal) fixed point, P , the saddle 2-cycle $\{Q_1, Q_2\}$, and its insets.¹ The points of the gray region go off to infinity. That is, their trajectories

1. By *inset* of P we mean the set of points attracted to P , also called the *stable set* of P .

FIGURE 4-3.

The attractor within the annular absorbing area.

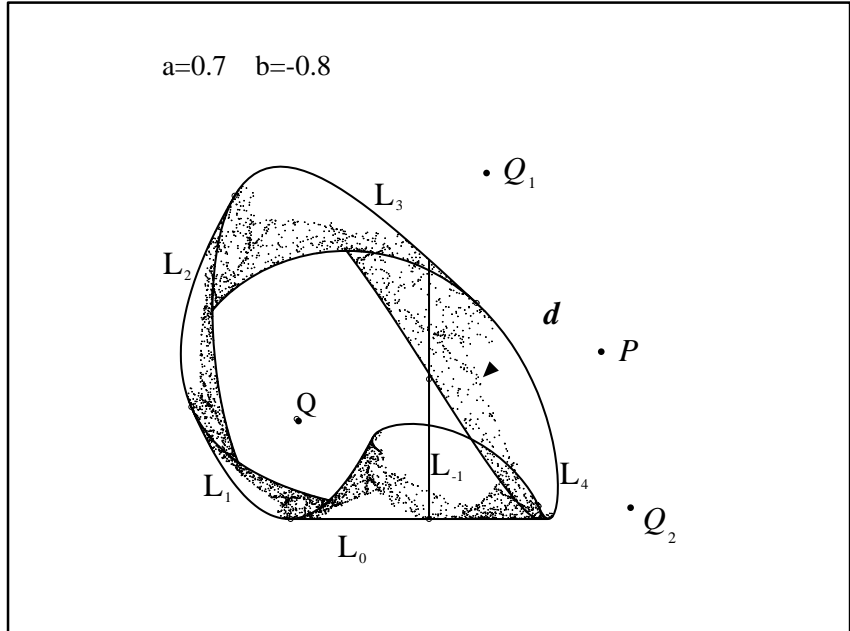


FIGURE 4-4.

Critical curves converging to the boundary of the attractor.

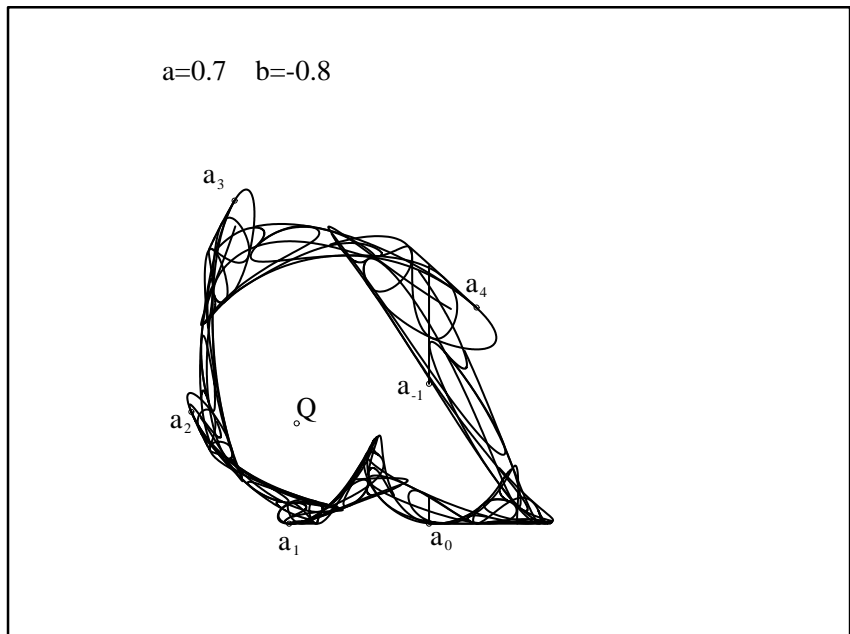
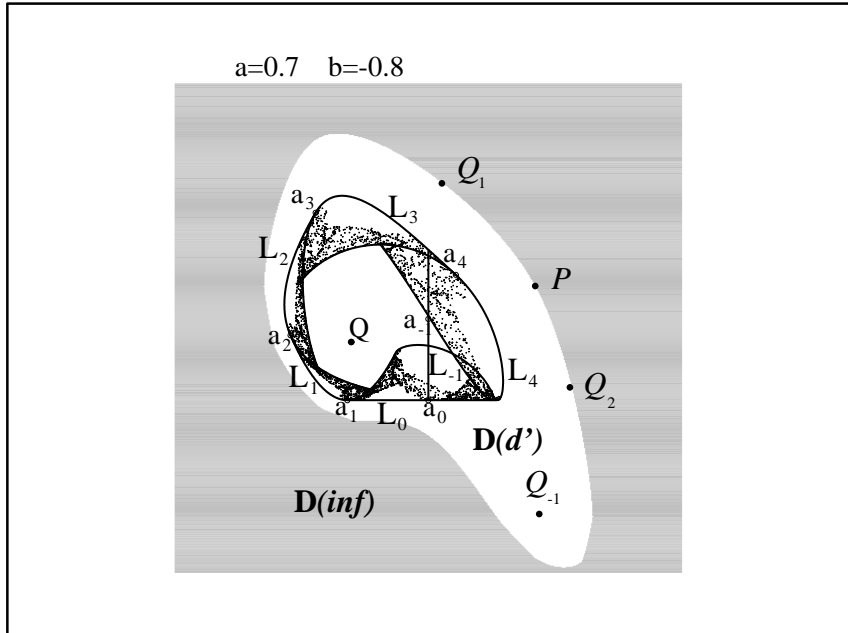


FIGURE 4-5.

The attractor in its basin.



are unbounded. We call this set the basin of infinity, $D(\infty)$. The white area $D(d')$ (excluding the fixed point Q and its rank 1 preimage Q_{-1} in Z_0) is the basin of the attractor d .

4.3 EXEMPLARY BIFURCATION SEQUENCE

In this first exemplary bifurcation sequence, we use the first family with $a = 0.7$, and decrease b from -0.4 to -1.0 , in seven stages.¹ For these values of b , our map always has two fixed points, P and Q , given by:

$$P: x = \frac{(1-a+\sqrt{\delta})}{2}, y = (1-a)x$$

$$Q: x = \frac{(1-a-\sqrt{\delta})}{2}, y = (1-a)x$$

where $\delta = (1-a)^2 - 4b$. Also, there is a 2-cycle, $\{Q_1, Q_2\}$.

Stage 1: $b = -0.4$

Here, the point Q , at about $(-0.5, -0.15)$, is an attractive fixed point. As b decreases, a Neimark-Hopf bifurcation occurs. The fixed point Q becomes a repellor and the curve Γ appears as an attractive invariant cycle, Γ (a closed curve mapped onto itself) that gradually increases in size as b continues to decrease.

Stage 2: $b = -0.5$

In Fig. 4-6, we see the point repellor Q within the attractive cycle Γ , and surrounding that, our first absorbing area, d' , shown shaded in Fig. 4-7. This area is mapped into itself, is bounded by arcs of critical curves, and is attractive (see Appendix 3.5 for the precise definition). In this case, the absorbing area is bounded by the arcs of the critical curves, L, L_1, L_2, L_3 , and L_4 . These bounding arcs are generated by successive iterations of the map, as we now describe.

1. We follow the paper BB.

FIGURE 4-6.

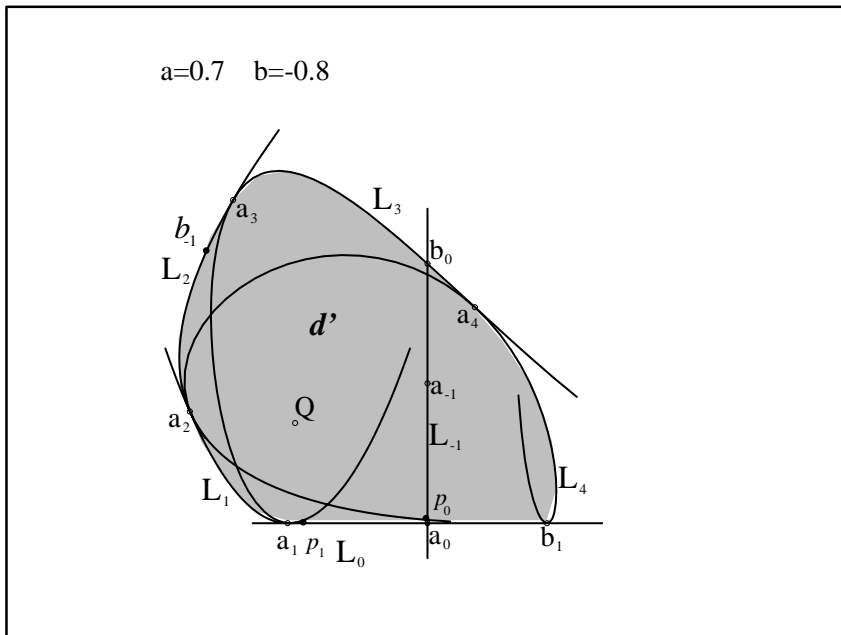


FIGURE 4-7.

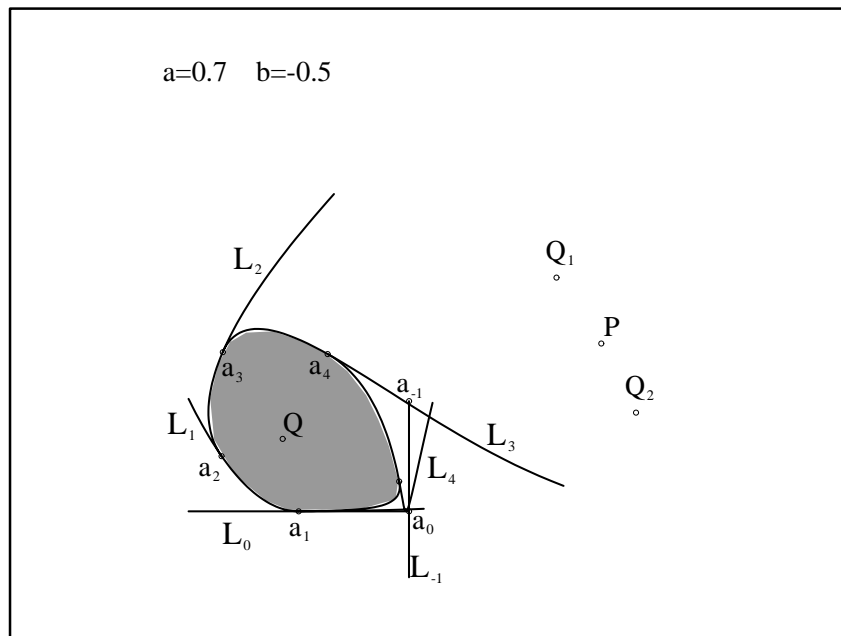
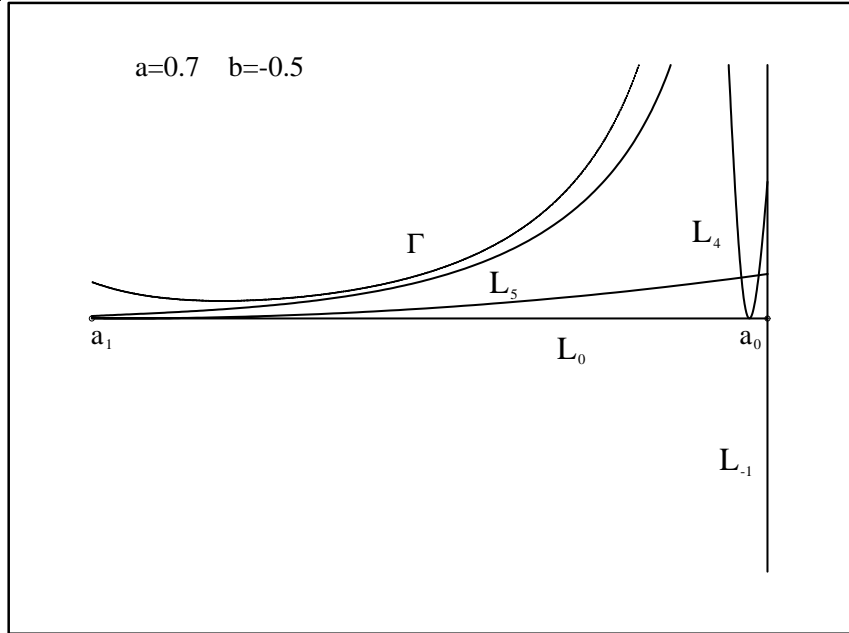


FIGURE 4-8.



Notice in Fig. 4-7, which shows the critical arcs in more detail, that L_{-1} and L are straight lines, crossing orthogonally in one point. Let a_0 denote this point, $(0, -0.5)$. Since it belongs to L , it has a unique preimage, a_{-1} , in L_{-1} . In this case a_{-1} is the origin $(0, 0)$.

Keeping the interval $a_{-1} a_0$ in mind, we now draw the successive images of the halfline of L_{-1} issuing from a_{-1} and containing a_0 , that is, issuing downwards. The fourth image, lying within L_3 , crosses the interval $a_{-1} a_0$, as shown in Fig. 4-7. At this event our constructive procedure ends, we have found an absorbing area, shown shaded in this figure. Further successive images of the segment converge on Γ , as shown in the blowup, Fig. 4-8. This procedure may be called *Procedure 1*. A related procedure is illustrated in the next stage.

As b continues to decrease, Γ expands further and eventually crosses L_{-1} .

Stage 3: $b = -0.6$

In this case Γ crosses L_{-1} in the two points p_0 and q_0 , as shown in Fig. 4-9. The wavy shape of Γ is a consequence of this crossing, and may be understood as follows.

Apply the map to the configuration shown in Fig. 4-9. The points p_0 and q_0 are mapped into the points p_1 and q_1 , also on Γ . The straight line segment of L_{-1} between p_0 and q_0 is mapped into the straight line segment of L between p_1 and q_1 . Because the map folds the plane two-to-one while moving L_{-1} to L , the curved segment of Γ between p_0 and q_0 is carried into the curved segment of Γ between p_1 and q_1 , which is above the line L . The transversal crossings of Γ through the line L_{-1} are mapped into tangencies of Γ with L at the points p_1 and q_1 . These tangencies are shown clearly in the enlargement, Fig. 4-10. This is a universal property of curves crossing L_{-1} : All crossings are mapped into tangencies, or contacts, because the map folds the plane at L_{-1} and maps the two sides of L_{-1} onto just one side of L . Hence, Γ obtains a wave from the image of its segment which has crossed L_{-1} .

Another effect of these tangencies is that Γ is now tangent to the boundary of the absorbing area d' identified in Stage 2 above, as shown in Fig. 4-11. This absorbing area may be found by the following method, called *Procedure 2*.

Consider the straight line segment S_{-1} from a_{-1} to a_0 in L_{-1} as above, and construct its successive images $a_m a_{m+1}$ by repeated applications of the map, until the first crossing with L_{-1} , in the point b_0 . See that the first image of S_{-1} , S_0 , is a straight line segment from a_0 to a_1 in L . The second image, S_1 , is a wave from a_1 to a_2 in L_1 , likewise S_2 in L_2 , S_3 in L_3 , and S_4 in L_4 . But S_4 crosses L_{-1} , and thus b_0 is found. Let A_{-1} denote the straight line segment from b_0 to a_0 in L_{-1} . Then A_{-1} contains the segment S_{-1} constructed just above, and its image A_0 is a straight line segment from b_1 to a_1 in L , containing S_0 . Now the curve segments A_0, S_1, S_2, S_3, B enclose the absorbing area d' , where B is the curve segment from $a_4 b_1$ within S_4 and L_4 , as shown in Fig. 4-12.

FIGURE 4-9.

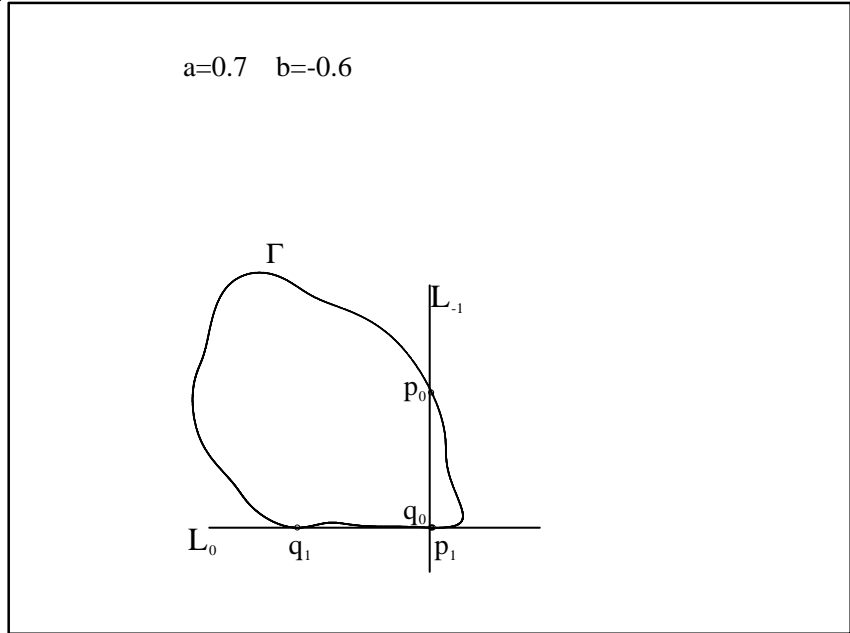


FIGURE 4-10.

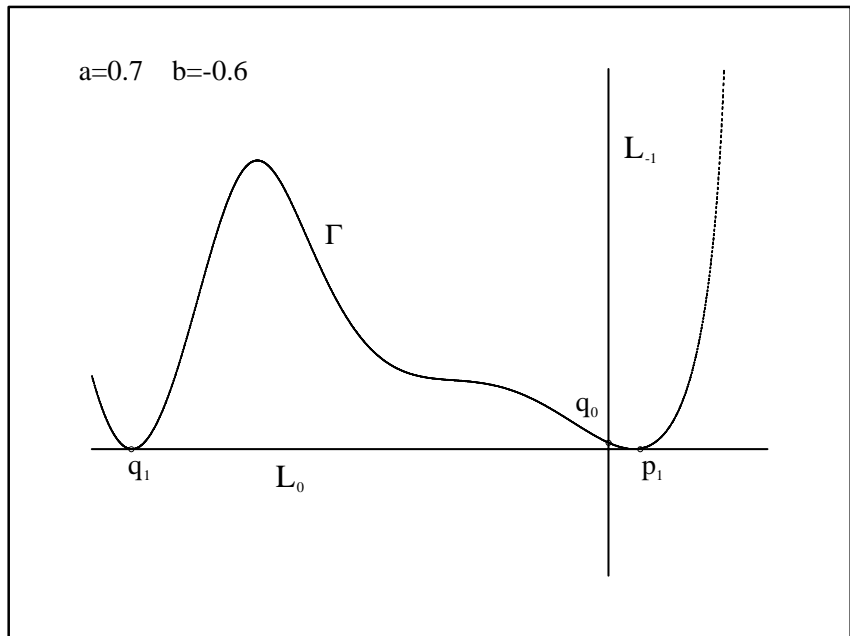


FIGURE 4-11.

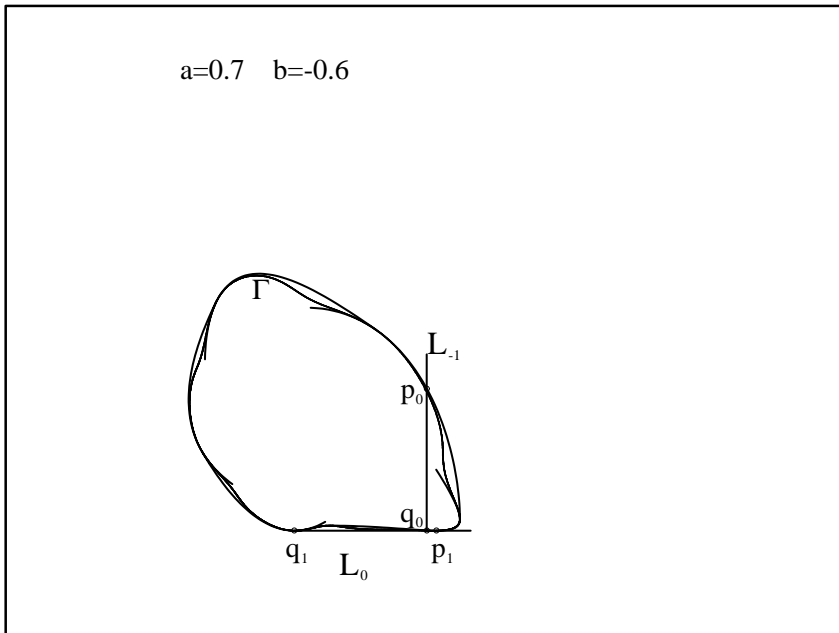


FIGURE 4-12.

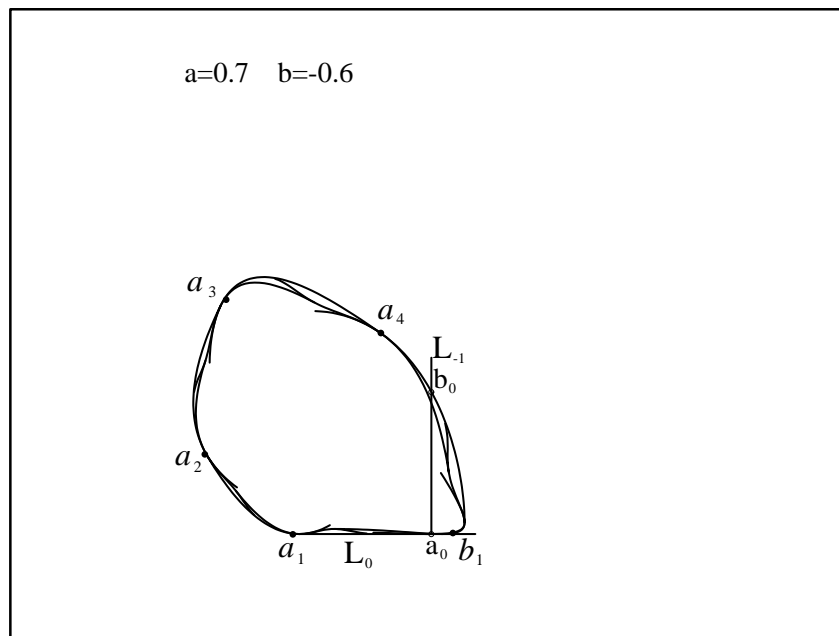
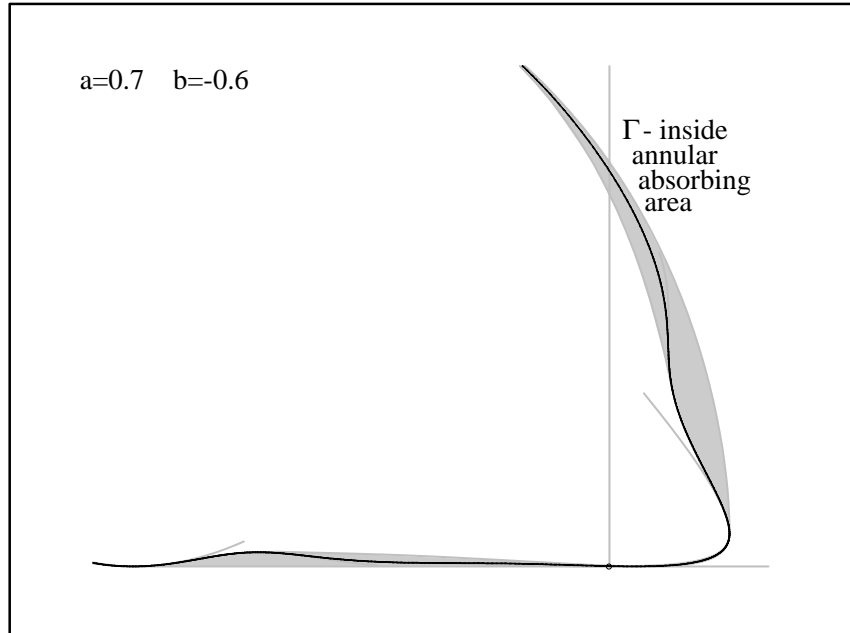


FIGURE 4-13.



At this stage, we may see yet another absorbing area, which is annular in shape. That is, it has a hole. This is shown bounded by shaded curves in the enlargement of Fig. 4-13. Its boundary is constructed of successive images of the straight line segment A_{-1} from b_0 to a_0 in L_{-1} . The attractive invariant curve, Γ , is tangent to the external boundary of this annular absorbing area, as well as to its interior boundary.

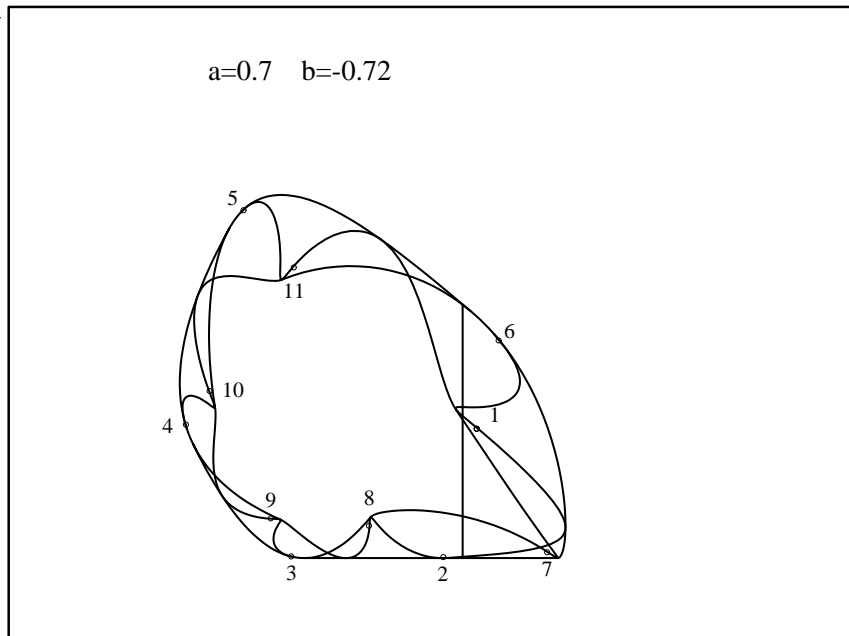
As b decreases further, many bifurcations occur in the dynamics within these absorbing areas. Probably they have not all been discovered, but we show just a few events in the remaining figures of this chapter.

Stage 4: $b = -0.72$

At this stage there is an attractive periodic cycle of period 11. The points of this cycle are labelled in iteration sequence in Fig. 4-14. This 11-cycle persists as b decreases further, through very many more bifurcations. The movie on the CD-ROM reveals an astonishing number of these, and many more have been observed, even in an interval of b values as narrow as 0.001.

FIGURE 4-14.

The attractive 11-cycle. Note the permutation sequence indicated by the numbers.

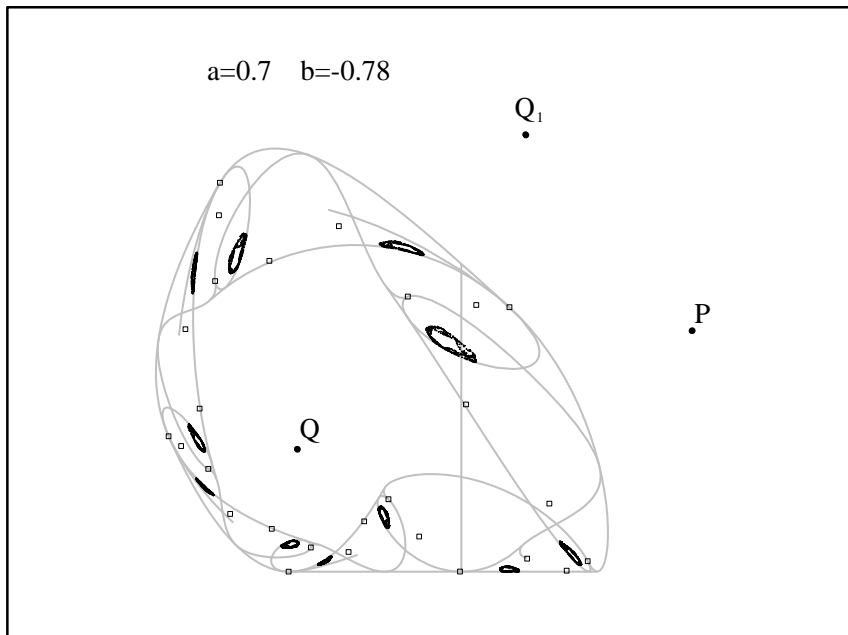


Stage 5: $b=-0.78$

At this stage we find two attractors coexisting within the annular absorbing area, a 28-cycle and an 11-piece chaotic attractor. These are shown in Fig. 4-15. Near $b = 0.798$, there is an explosion to a chaotic attractor filling an annular absorbing area.

FIGURE 4-15.

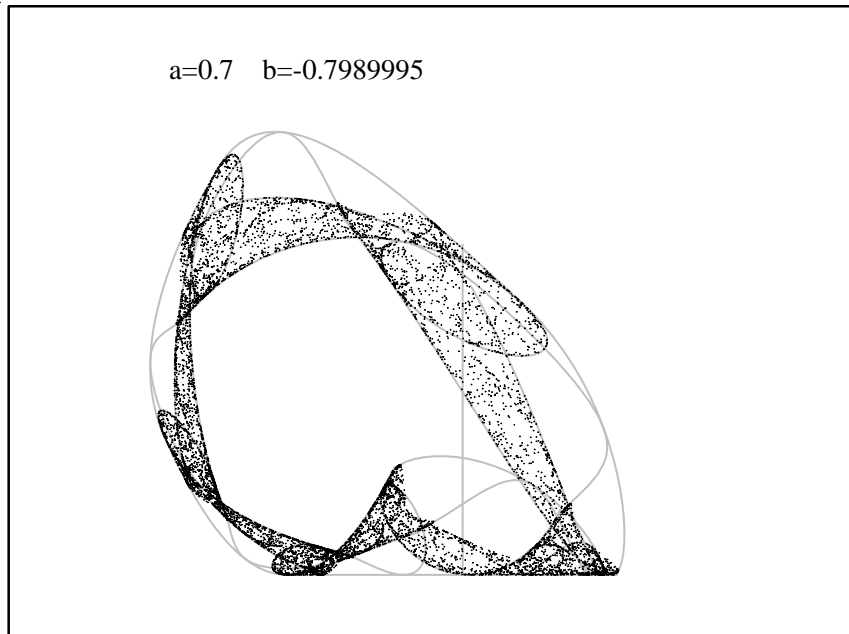
The 11-cyclic chaotic attractor. The permutation of the pieces follows the numbering of Fig. 4-14.



Stage 6: $b = -0.7989995$

Fig. 4-16 shows the chaotic attractor, bounded by critical curves. Passing below $b = -0.8$, there are a number of additional bifurcations which have been studied on the research frontier. Some of them will be described later in this book. Approaching $b = -1.0$, further explosions are found.

FIGURE 4-16.



Stage 7: $b = -0.975$

The densely dotted region of Fig. 4-17 is a large chaotic attractor, an annular chaotic area, d . The frontier, F , of its basin of attraction, includes the inset of the 2-cycle, $\{Q_1, Q_2\}$. The boundary of d is very near F . This figure shows that the critical curves (on the boundary of the former chaotic area) are about to touch (and then to cross) the inset of the 2-cycle.

The enlargement of Fig. 4-18 shows that, in addition, a contact of the frontier, F , with the boundary on L is about to occur. This contact bifurcation, described in Chapter 7, has the effect of destroying the chaotic attractor, or rather, of transforming it into a chaotic repeller. Now, almost all of the trajectories diverge to infinity, except for a Cantor set surviving inside the former chaotic area.

A rough idea of the basin of infinity, $D(\infty)$, is shown in Fig. 4-19 as a black area. The basin of infinity includes infinitely many holes in the former absorbing area, d' , only a few of which are shown in this figure. The light area is the basin of attraction of the attractor d . An enlargement is shown in Fig. 4-20.

FIGURE 4-17.

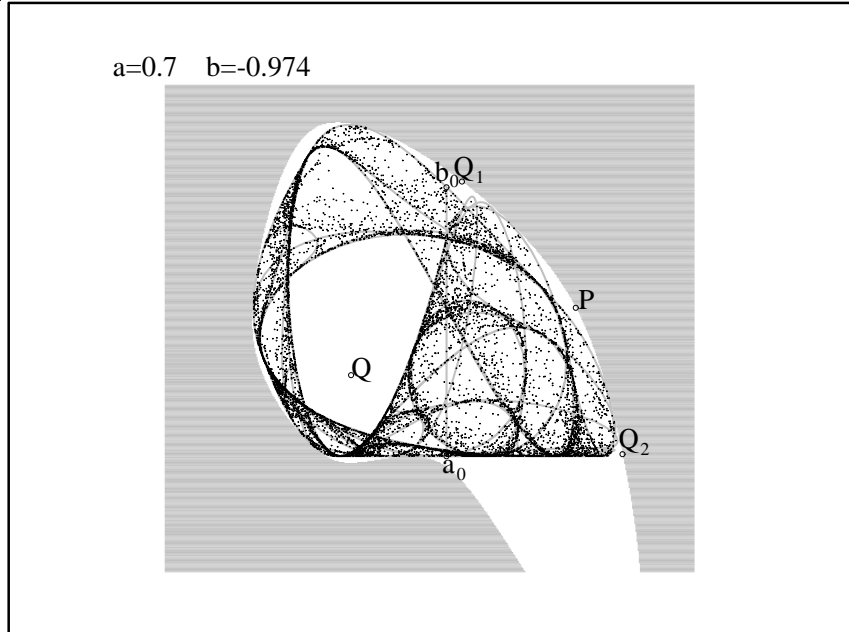


FIGURE 4-18.

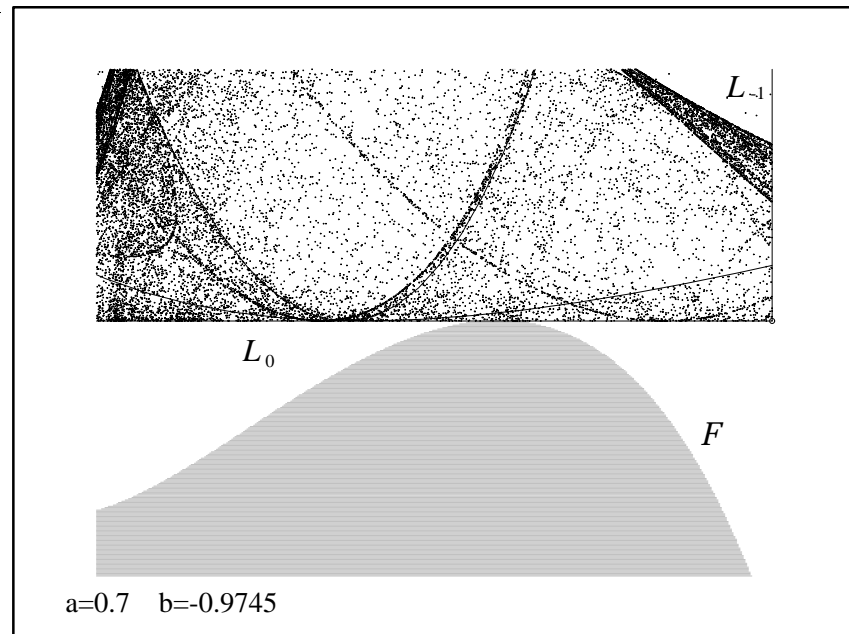


FIGURE 4-19.

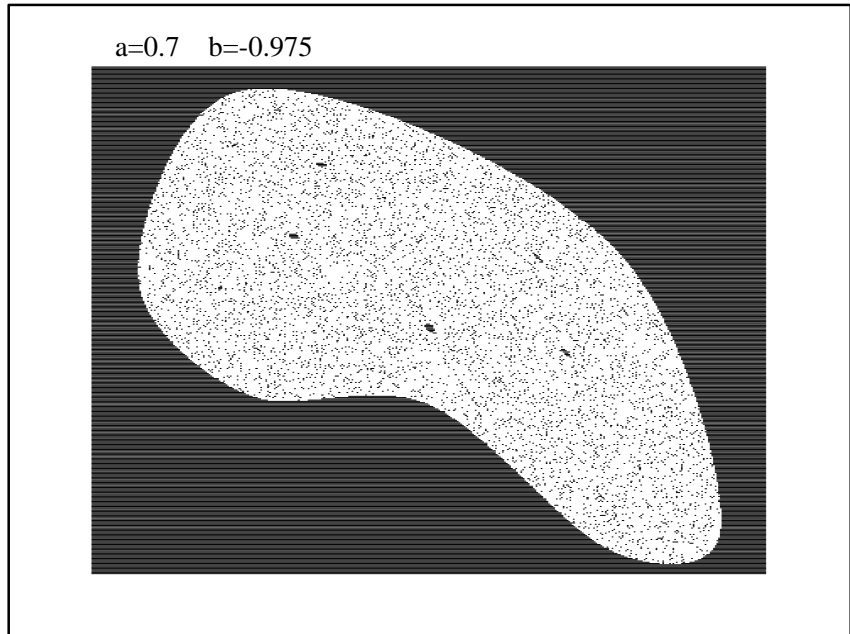


FIGURE 4-20.

